Spatial Sigma-Delta Signal Acquisition for Wideband Beamforming Arrays

Ryan M. Corey and Andrew C. Singer
University of Illinois at Urbana-Champaign

***Abstract*—We consider spatial and spatio-temporal sigma-delta modulation structures for wideband signal acquisition with dense sensor arrays. Using closely arranged sensors, the array oversamples the signal in space and applies coarse quantization to each sensor output. A sigma-delta structure propagates quantization noise between sensors to shape the noise in space, just as a time-domain sigma-delta converter shapes noise in frequency. The spatially shaped noise is then filtered by a delay-and-sum beamformer. In this work, we also introduce higher-order sigma-delta structures and hybrid space-time architectures that can achieve greater noise shaping in both space and time. The coarsely quantized sigma-delta structure can be used to build high-resolution arrays with lower power and complexity.**

I. Introduction

Sensor arrays, which can be used for directional signal processing, are essential in many communication, acoustic, and imaging applications [1]. Recent research, particularly in the area of wireless communication, has explored the benefits of "massive" arrays [2]; that is, arrays with large numbers of elements. These arrays offer improved spatial resolution, among other benefits, but require more mixed-signal hardware resources and computational power to process the large number of input signals. In this work, we propose an efficient array design with a large number of sensors that each produce a low-resolution (e.g., 1 bit per sample) data stream. These streams can be combined in a delay-and-sum beamformer to form a high-resolution output signal.

There has been some recent work on coarsely quantized arrays for communication applications. Low-resolution analog-to-digital converters (ADCs) are advantageous for large arrays because they have lower power and complexity requirements than higher-resolution converters. In [3], a the authors considered a wideband multiple-input multiple-output array with single-bit ADCs. The coarse quantization caused minimal degradation in channel capacity in the low signal-to-noise ratio regime. There have been a number of studies [4], [5], [6], [7] on channel estimation based on single-bit measurements; the spatial redundancy of large arrays and sparsity of the channels helps to compensate for the reduced resolution of the converters. The single-bit measurements can also be used directly for some spatial signal processing applications, such as direction-of-arrival estimation [8]. Low-resolution converters can be especially advantageous in compact arrays with closely spaced elements [9], which are the subject of this work.

This work was supported in part by Systems on Nanoscale Information fabriCs (SONIC), one of the six STARnet centers sponsored by MARCO and DARPA. This material is based upon work supported by the National Science Foundation Graduate Research Fellowship Program under Grant Number DGE-1144245.

Single-bit signals have long been common in oversampled ADCs, such as the celebrated sigma-delta converter [10]. A sigma-delta modulator uses a low-resolution quantizer with a feedback loop to shape the quantization noise spectrum such that quantization effects are shifted to higher frequencies outside the signal band. These errors are removed by a discrete-time filter during decimation. Since a delay-and-sum beamformer is essentially a discrete filter sampled in space rather than time, it should be possible to apply the same error-shaping technique to sensor arrays. In a conventional linear beamforming array, the spacing between sensors is chosen to be close to half of the shortest wavelength in the signal of interest – the spatial equivalent of the Nyquist rate. In a spatially oversampled array, the spacing is much smaller than a half wavelength. Noise shaping is accomplished by propagating quantization errors from one sensor to the next. These errors accumulate at high spatial frequencies and are filtered by the delay-and-sum operation.

There have been a few previous studies on spatial sigma-delta noise shaping. In [11], the authors proposed a joint space-time sigma-delta vector quantization scheme for transmit arrays. However, the design resembles a conventional time-domain modulator as quantization errors are fed back in time, not in space. The nearest precedents to the present work are [12], [13] and related papers, in which the complex weights (phase shifts) of a phased array are coarsely quantized and the quantization errors of the weights are shaped by spatial feedback. There are two major differences between [13] and this work: first, we consider sigma-delta modulation of the received signal itself rather than of the phase shifts of a phased array; second, we consider wideband delay-and-sum beamforming rather than narrowband phased-array beamforming.

Our focus here will be on low-frequency applications, such as microphone arrays, in which the delay-and-sum beamforming operations are performed directly on the information signal, avoiding the problems associated with operation on a signal modulated by a high-frequency carrier. In these systems, beamforming and other spatial processing operations, such as direction-of-arrival estimation and source separation, can be performed in the digital domain using the sampled data [14]. The proposed architecture applies sigma-delta modulation to the received signal, propagating quantization errors between adjacent sensors and producing a set of coarsely quantized output signals. After analyzing the noise-shaping characteristics of the first-order spatial sigma-delta structure, we will consider higher-order modulators and hybrid time-space noise shaping, which can further improve resolution for wideband systems.

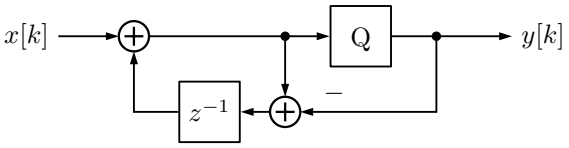

Figure 1. A first-order sigma-delta modulator in the time domain. The "Q" block is a low-resolution quantizer.

II. Array Model

Sensor array processing is analogous in many ways to discrete-time signal processing: in an array, signals are sampled at regular intervals in space (or with a particularly convenient spatial pattern) and filtered to isolate signals from a particular direction. This analogy is valuable in understanding spatial sigma-delta modulation. Consider a linear array of N elements spaced distance d apart. For simplicity, we assume plane wave propagation in a dispersionless linear medium. Let $x_n(t)$ denote the continuous-time signal received at sensor n for $n = 0, \ldots, N-1$, and let $X_n(\Omega)$ be its continuous-time Fourier transform (CTFT). Let $r = \frac{d}{c}\cos\theta$ be the relative time delay between sensors for signals arriving at angle θ relative to the array axis. Thus, $r = \frac{d}{c}$ at endfire and 0 at broadside. The output $\tilde{x}_r(t)$ of such a delay-and-sum beamformer steered to an angle corresponding to delay r is given by

$$\tilde{x}_r(t) = \frac{1}{N}\sum_{n=0}^{N-1} x_n(t - nr). \tag{1}$$

In the CTFT domain, the beamformer output is

$$\tilde{X}_r(\Omega) = \frac{1}{N}\sum_{n=0}^{N-1} X_n(\Omega)\, e^{-j\Omega nr}, \tag{2}$$

which is analogous to a discrete-time Fourier transform of the narrowband signals $\{X_n(\Omega)\}_{n=0}^{N-1}$ with $r\Omega$ as the spatial frequency.

III. Sigma-Delta Architecture

A. Sigma-delta modulation

Figure 1 shows a first-order sigma-delta modulation structure. A discrete-time, continuous-valued input sequence $x[k]$ is quantized to produce a discrete-valued output sequence $y[k]$. The quantization operation is modeled as a linear additive noise process so that $Q(u[k]) = u[k] + q[k]$, where $q[k]$ is the continuous-valued quantization noise signal. To shape the quantization noise at the output, each $q[k]$ is fed back and subtracted from the next input. The output of the time-domain modulator can thus be written

$$\begin{aligned} y[k] &= Q(x[k] - q[k-1]) && (3)\\ &= x[k] + q[k] - q[k-1]. && (4)\end{aligned}$$

Under this linear model, the modulator applies unity gain to the signal but a highpass filter, $H(z) = 1 - z^{-1}$, to the quantization noise. This highpass filter is called the noise transfer function (NTF). In a sigma-delta ADC, the oversampled coarsely quantized sequence $y[k]$ would then be lowpass filtered and decimated to produce a more finely quantized Nyquist-rate signal.

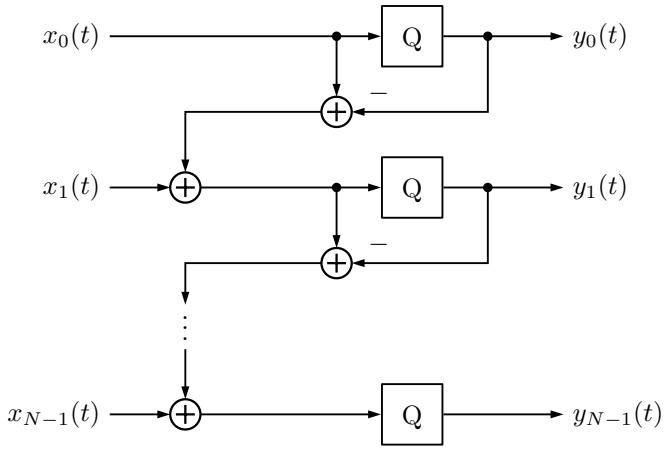

Figure 2. A first-order spatial sigma-delta array with N elements.

B. First-order spatial sigma-delta structure

Figure 2 shows a first-order spatial sigma-delta array. It is similar to the time-domain structure of Figure 1 except that time delays are replaced by spatial propagation to the next element. Furthermore, due to the finite extent of the array, the input is defined only for $0 \le n \le N-1$. This system is modeled by the input-output relation

$$y_n(t) = x_n(t) + q_n(t) - q_{n-1}(t), \tag{5}$$

where $q_n(t)$ is the noise introduced by the n^{th} quantizer for $0 \le n \le N-1$ and $q_n(t) = 0$ for $n < 0$. The output of a delay-and-sum beamformer steered to r is then

$$\begin{aligned} \tilde{y}_r(t) &= \frac{1}{N}\sum_{n=0}^{N-1} y_n(t - nr) && (6)\\ &= \frac{1}{N}\sum_{n=0}^{N-1} [x_n(t-nr) + q_n(t-nr) - q_{n-1}(t-nr)] && (7)\\ &= \tilde{x}_r(t) + \tilde{q}_r(t) - \frac{1}{N}\sum_{n=0}^{N-2} q_n(t-(n+1)r) && (8)\\ &= \tilde{x}_r(t) + \tilde{q}_r(t) - \tilde{q}_r(t-r) + \frac{1}{N} q_{N-1}(t-Nr). && (9)\end{aligned}$$

The noise shaping effect can be seen when the output is written in the frequency domain:

$$\begin{aligned} \tilde{Y}_r(\Omega) &= \tilde{X}_r(\Omega) + (1 - e^{-j\Omega r})\tilde{Q}_r(\Omega) \\ &\quad + \frac{1}{N} Q_{N-1}(\Omega) e^{-j\Omega Nr}. && (10)\end{aligned}$$

Note that due to the finite length of the array, the quantization noise introduced by the last sensor is not shaped. For each other noise signal, the NTF is $H_r(\Omega) = 1 - e^{-j\Omega r}$, which has gain

$$\begin{aligned} |H_r(\Omega)|^2 &= \left|1 - e^{-j\Omega r}\right|^2 && (11)\\ &= 4\sin^2\left(\frac{\Omega r}{2}\right) && (12)\\ &= 4\sin^2\left(\frac{d}{2c}\Omega\cos\theta\right). && (13)\end{aligned}$$

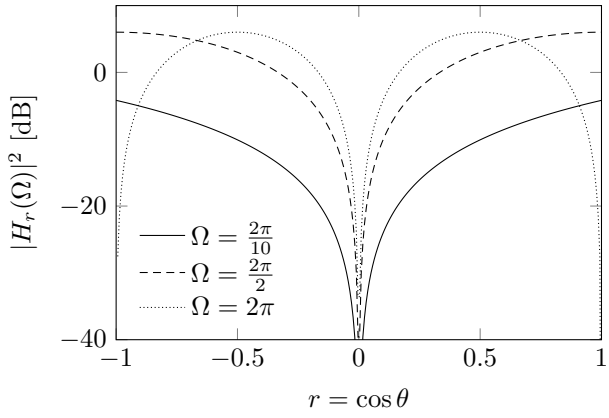

Figure 3. The spatial noise transfer function (12) of a first-order spatial sigma-delta modulator for an array with $d/c = 1$. The noise is most strongly attenuated near broadside.

For a fixed temporal frequency Ω, $H_r(\Omega)$ shapes the noise to larger values of r, as shown in Figure 3. Thus, this array configuration is most useful for steering directions close to broadside ($r = 0$). The spatial noise shaping effect is strongest for frequencies much smaller than c/d. Indeed, for fixed nonzero r, (12) shifts quantization noise to higher temporal frequencies, much like a time-domain sigma-delta modulator.

C. Higher-order modulation

The first-order sigma-delta structure of Figure 1 is rarely used in high-resolution applications, such as audio recording. Its noise-shaping power can be improved using additional sigma-delta stages. For example, a second-order sigma-delta modulator has the input-output model

$$y[k] = x[k] + q[k] - 2q[k-1] + q[k-2], \qquad (14)$$

which corresponds to $H(z) = (1 - z^{-1})^2$. This transfer function provides stronger high-frequency noise shaping, further reducing the output error in the signal band. The same approach can be used to improve the spatial sigma-delta structure. The second-order spatial sigma-delta modulator, shown in Figure 4, is analogous to the time-domain modulator except that the last sensor uses a first-order structure. The system has the input-output model

$$y_n(t) = \begin{cases} x_n(t)+q_n(t)-2q_{n-1}(t)+q_{n-2}(t), & 0 \le n \le N-2 \\ x_n(t)+q_n(t)-q_{n-1}(t)+q_{n-2}(t), & n = N-1. \end{cases} \qquad (15)$$

Using this model, the beamformer output is given by

$$\begin{aligned} \tilde{Y}_r(\Omega) &= \tilde{X}_r(\Omega) + (1-e^{-j\Omega r})^2 \frac{1}{N} \sum_{n=0}^{N-3} Q_n(\Omega) e^{-j\Omega n r} \\ &\quad + \frac{1}{N}(1-e^{-j\Omega r}) Q_{N-2}(\Omega) e^{-j\Omega(N-2)r} \\ &\quad + \frac{1}{N} Q_{N-1}(\Omega) e^{-j\Omega(N-1)r} \qquad (16) \\ &= \tilde{X}_r(\Omega) + (1-e^{-j\Omega r})^2 \tilde{Q}_r(\Omega) \\ &\quad + \frac{1}{N}(1-e^{-j\Omega r}) Q_{N-2}(\Omega) e^{-j\Omega(N-1)r} \\ &\quad + \frac{1}{N}(2-e^{-j\Omega r}) Q_{N-1}(\Omega) e^{-j\Omega N r}. \qquad (17) \end{aligned}$$

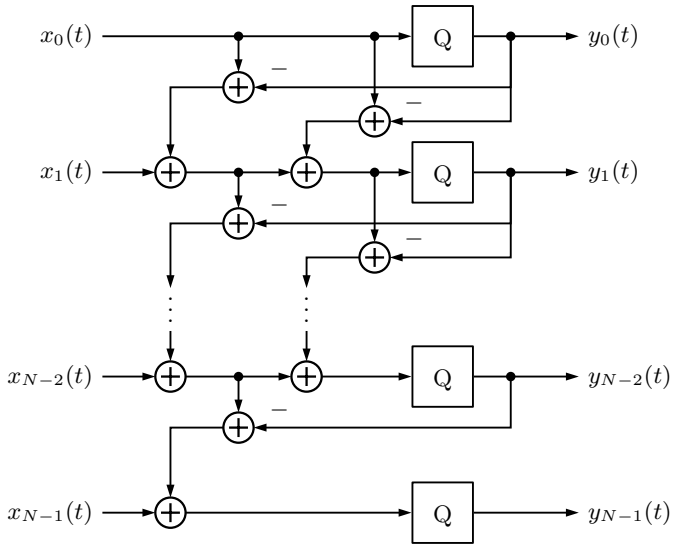

Figure 4. A second-order spatial sigma-delta modulator. The final stage is first-order.

The noise transfer function for the second-order modulator is $(1 - e^{-j\Omega r})^2$, which has gain $16 \sin^4(\Omega r/2)$. Because the final sensor uses a first-order modulator, the penultimate noise signal, $q_{N-2}(t)$, has first-order shaping, and the noise from the final quantizer, $q_{N-1}(t)$, is not shaped. Thus, the first- and second-order modulators have identical noise suppression at broadside, but the second-order modulator provides stronger spatial shaping. Third- and higher-order noise shaping designs are also possible using modified feedback architectures to prevent instability [10].

IV. Spatio-Temporal Architectures

A. Modulation in sampled systems

The analysis in the previous section assumes that the signals are acquired and processed in continuous time and that the integrators and quantizers work instantaneously. A more realistic model must account for hold times at the quantizers and between stages. For simplicity, assume that all components are controlled by a single clock with period τ. Figure 5 shows a first-order spatial sigma-delta modulator with latches in front of each quantizer.

Using the additive linear quantization noise model as before, the system in Figure 5 is modeled by

$$y_n(t) = x_n(t-\tau) + q_n(t) - q_{n-1}(t-\tau). \qquad (18)$$

The beamformer output is then

$$\begin{aligned} \tilde{Y}_r(\Omega) &= \tilde{X}_r(\Omega) e^{-j\Omega\tau} + (1-e^{-j\Omega(\tau+r)}) \tilde{Q}_r(\Omega) \\ &\quad + \frac{1}{N} Q_{N-1}(\Omega) e^{-j\Omega(\tau+Nr)}. \qquad (19) \end{aligned}$$

Notice that the target signal now has a delay of one sample and the spatial NTF has been shifted by τ. Thus, the minimum no longer occurs at broadside.

The second-order sampled modulator is similar to the system in Figure 4, with latches in front of the quantizer inputs and also on the propagation path of the first integration stage. The resulting NTF is $(1-e^{-j\Omega(r+\tau)})^2$ for all but the final two quantization noise signals.

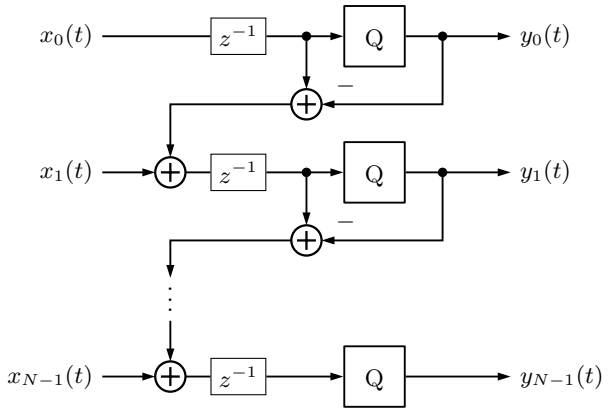

Figure 5. A first-order spatial sigma-delta modulator in a sample-and-hold system. The z^{-1} blocks represent time delays of τ.

B. Symmetric spatial sigma-delta structure

The spatial sigma-delta structure is in some ways more flexible than a time-domain sigma-delta modulator. For example, the noise-shaping filter need not be causal. Consider the second-order system shown in Figure 6. Quantization noise is propagated both forward and backward in space. The first and last stages have first-order shaping and all other stages have second-order shaping. The propagation delays are necessary in this structure to prevent instantaneous feedback loops.

The quantizer outputs are modeled as

$$y_n(t) = \begin{cases} x_n(t-\tau)+q_n(t)-q_{n+1}(t-\tau), & n=0 \\ x_n(t-\tau)+q_n(t)-q_{n-1}(t-\tau) & \\ \quad -q_{n+1}(t-\tau)+q_n(t-2\tau), & 1\le n\le N-1 \\ x_n(t-\tau)+q_n(t)-q_{n-1}(t-\tau), & n=N-1. \end{cases} \tag{20}$$

The beamformer output is modeled as

$$\begin{aligned} \tilde{Y}_r(\Omega) =& \tilde{X}_r(\Omega)e^{-j\Omega\tau}+(1-e^{-j\Omega(\tau+r)})(1-e^{-j\Omega(\tau-r)})\tilde{Q}_r(\Omega) \\ &+ \frac{1}{N}(1-e^{-j\Omega(\tau+r)})Q_0(\Omega)e^{-j\Omega(\tau-r)} \\ &+ \frac{1}{N}(1-e^{-j\Omega(\tau-r)})Q_{N-1}(\Omega)e^{-j\Omega(\tau+Nr)}. \end{aligned} \tag{21}$$

The NTF gain for the central stages of the second-order symmetric modulator is $16\sin^2(\frac{\Omega}{2}(\tau+r))\sin^2(\frac{\Omega}{2}(\tau-r))$. Figure 7 compares the noise shaping performance of the second-order feed-forward structure with and without propagation delays and the symmetric second-order structure. The symmetric response may be preferable in some applications. It is particularly advantageous in small-N arrays because there are no unshaped noise signals in the beamformer output.

Spatial noise shaping can be applied to other array configurations as well. For example, the bidirectional error propagation in Figure 6 could be used in a circular sensor array. In such an array, the time delays between elements are nonuniform, leading to more complicated noise-shaping behavior.

C. Cascaded space-time architectures

The spatial sigma-delta structures presented in this paper shape the quantization noise signals by first propagating the noise through space, then passing the resulting outputs through a delay-and-sum beamformer. If the quantization noise signals were truly noiselike, with flat frequency spectra, then the error in the beamformer output would be concentrated at high frequencies. However, because the inputs to the sensors in an array are typically strongly correlated, the quantization noise signals may also be correlated. As a result, the output error spectrum may have strong low-frequency components. Figure 8 shows the average unshaped quantization noise spectrum, $Q_n(\Omega)$, for several modulator structures based on the simulation data from Section V. With no modulation, the quantization noise is concentrated near the signal band. The unshaped noise in the spatial modulator is similarly concentrated at low frequencies. The noise signal in the temporal modulator, however, has a flatter spectrum even before shaping.

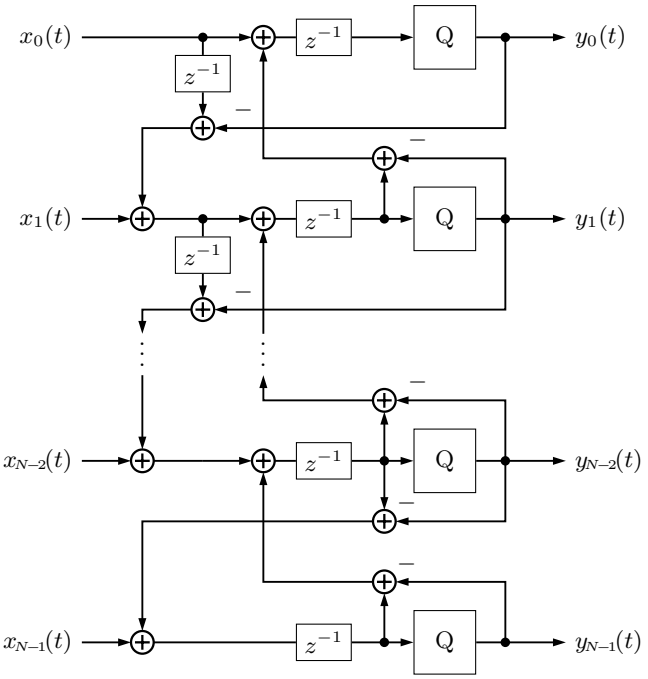

Figure 6. A second-order symmetric spatial sigma-delta modulator. The first and last stages are first-order.

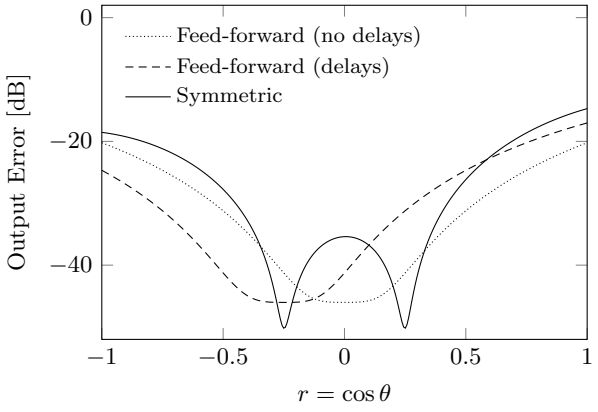

Figure 7. Example output error curves for second-order feed-forward and symmetric modulators with sample-and-hold delays. The curves were generated using $N = 200$, $\frac{d}{c} = 1$, $\Omega = \frac{2\pi}{5}$, $\tau = \frac{1}{4}$ and $|Q_n(\Omega)|^2 = 0$ dB.

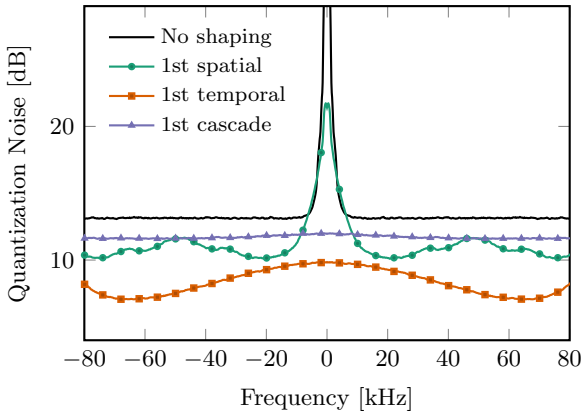

Figure 8. Average unshaped quantization error power spectrum, $|Q_n(\Omega)|^2$, for several modulator structures using a single-bit quantizer. The noise power is measured relative to the error-free output power.

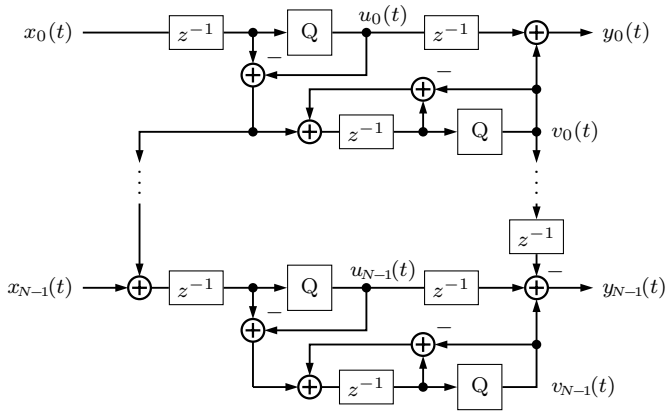

Figure 9. Cascaded spatio-temporal architecture. The quantization noise signal from each spatial modulator stage is shaped by a time-domain sigma-delta modulator.

To reduce the temporal correlations in the quantization error signal, we can incorporate traditional time-domain sigma-delta modulation. Any of the spatial modulators presented in this paper can be modified using a cascade structure, sometimes referred to as a multi-stage noise shaping (MASH) modulator. The cascade architecture, in which the quantization noise of the first stage is modulated by a second stage and then subtracted, is often used in higher-order time-domain converters to prevent instability. Figure 9 shows a first-order spatial modulator cascaded with a first-order temporal modulator. For simplicity, it is assumed that both stages operate with sample period τ, though a practical system may use different rates.

Let $u_n(t)$ be the output of the spatial stage and let $q_n^*(t)$ be the quantization noise of that stage. The negative of this noise is used as the input to the temporal stage. Let $v_n(t)$ and $q_n(t)$ be the output and quantization noise, respectively, of the second stage. The two stages of Figure 9 are governed by the equations

$$u_n(t) = x_n(t-\tau) + q_n^*(t) - q_{n-1}^*(t-\tau) \quad (22)$$
$$v_n(t) = -q_n^*(t-\tau) + q_n(t) - q_n(t-\tau). \quad (23)$$

Thus, $u_n(t)$ is a delayed approximation of $x_n(t)$ and $v_n(t)$ is a delayed approximation of $-q_n^*(t)$. Finally, the $v_n(t)$ signals are combined so as to cancel the $q_n^*(t)$ terms in the output:

$$\begin{aligned} y_n(t) &= u_n(t-\tau) + v_n(t) - v_{n-1}(t-\tau) \quad (24)\\ &= x_n(t-2\tau) + q_n(t) - q_n(t-\tau) \\ &\quad -q_{n-1}(t-\tau) + q_{n-1}(t-2\tau). \quad (25)\end{aligned}$$

The delay-and-sum beamformer output is then

$$\begin{aligned}\tilde{Y}_r(\Omega) =& \tilde{X}_r(\Omega)e^{-j\Omega 2\tau} + (1-e^{-j\Omega\tau})(1-e^{-j\Omega(\tau+r)})\tilde{Q}_r(\Omega) \\ &+ \frac{1}{N}(1-e^{-j\Omega\tau})Q_{N-1}(\Omega)e^{-j\Omega(\tau+Nr)}. \quad (26)\end{aligned}$$

The noise shaping effect of the cascade structure is stronger than that of the spatial modulator alone. Furthermore, as Figure 8 shows, the cascade has a nearly flat unshaped quantization noise spectrum and so does not exhibit the strong low-frequency error components present in the spatial modulator output.

If the spatial stage were a second-order feed-forward modulator, then the output stage would be modified so that

$$y_n(t) = u_n(t-\tau) + v_n(t) - 2v_{n-1}(t-\tau) + v_{n-2}(t-2\tau), \quad (27)$$

and the resulting transfer function would be $(1-e^{-j\Omega\tau})(1-e^{-j\Omega(\tau+r)})^2$ for all but the final two stages. Similarly, the output stage for the symmetric modulator would be

$$\begin{aligned} y_n(t) &= u_n(t-\tau) + v_n(t) - v_{n-1}(t-\tau) \quad (28)\\ &\quad -v_{n+1}(t-\tau) + v_n(t-2\tau), \quad (29)\end{aligned}$$

and the noise transfer function would be $(1-e^{-j\Omega\tau})(1-e^{-j\Omega(\tau+r)})(1-e^{-j\Omega(\tau-r)})$ for all but the first and last stages.

V. Simulations

The noise shaping responses derived in the previous sections are based on a linear model of the quantization noise feedback loop. Like any nonlinear modulation scheme, the spatial and spatio-temporal sigma-delta architectures are best evaluated using real or simulated signals. In this section, we simulate a spatial sigma-delta microphone array using recorded speech data. The array consists of $N = 50$ linear isotropic elements spaced $d = 1$ cm apart. The propagation speed is assumed to be 330 m/s, giving an interelement time delay of $\frac{d}{c} = 30.3$ μs. The sample rate is $f_s = 240$ kHz, giving $\tau = 4.17$ μs. The target signal is a one second recording of the author speaking the phrase "sigma-delta". This signal originates from $\theta = 90°$, at the array broadside. Four speech babble signals are placed at 30°, 60°, 120°, and 150°. Each microphone is subject to independent additive white Gaussian noise with power 10 dB below the signal level. If the frequency range of interest is 0 to 3 kHz, then the spatial oversampling ratio is 5.5. The quantizer is a single bit.

Figures 10, 11, and 12 show the error power at the beamformer output for several architectures. The error power, $|\tilde{Y}_r - \tilde{X}_r|^2$, is presented in dB relative to the error-free output power. The dotted curves show the expected output error power based on the noise transfer functions derived above, assuming that the quantization noise samples are independent and uniformly distributed on $[-1, 1]$. The solid black curve shows the error spectrum with no modulation.

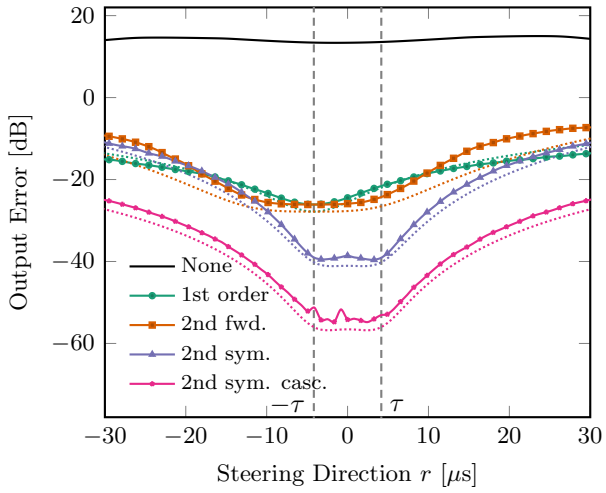

Figure 10. Passband output error power, relative to the error-free output power, as a function of steering direction. The r-axis covers the visible region between $-\frac{d}{c}$ and $+\frac{d}{c}$. The dotted curves show the predicted error.

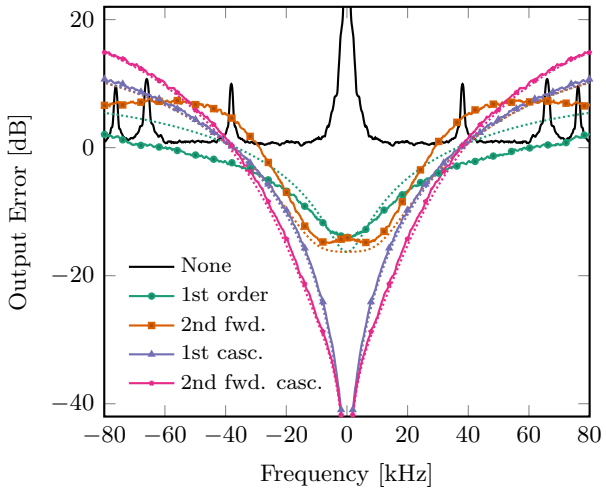

Figure 11. Output error power spectrum, relative to the error-free output power, of the simulated array steered to broadside. The dotted curves show the predicted error.

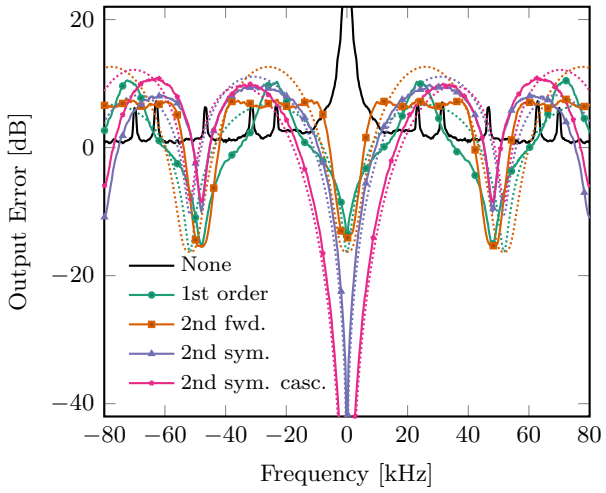

Figure 12. Output error power spectrum, relative to the error-free output power, of the simulated array steered to $\theta = 60°$. The dotted curves show the predicted error.

Figure 10 shows the error power as a function of steering direction for the first- and second-order feed-forward modulators, the second-order symmetric modulator, and the second-order symmetric cascade. All the modulators shape the quantization noise away from broadside, with a stronger shaping effect for higher-order modulators. Notice that the first- and second-order curves are minimized at $r = -\tau$, while the symmetric structures have minima at $\pm\tau$. The second-order symmetric modulator outperforms the second-order forward modulator near broadside because the symmetric modulator shapes all N noise signals, while the feed-forward modulator does not shape the noise introduced by the final quantizer.

Figure 11 shows the output error power spectrum when the array is steered to broadside for the first- and second-order forward modulators with and without a cascaded temporal stage. For the two cascaded architectures, the simulated performance closely matches the predictions based on the linear model. The spatial-only architectures exhibit unexpectedly large error in the passband. This discrepancy is due to the strong low-frequency components of the unshaped quantization noise spectrum. The temporal stage of the cascade flattens this noise spectrum before shaping.

Figure 12 shows the error spectrum when the array is steered to 60° for the same architectures as Figure 10. At this angle, the error is shaped into relatively lower frequencies than at broadside. The second-order feed-forward modulator, for example, places significant error around 10 kHz, which is audible to human listeners. The array performance could be improved by increasing the spatial oversampling ratio; that is, by decreasing the microphone spacing. Notice that the symmetric modulator attenuates the noise more strongly than the feed-forward modulator near zero frequency, even away from broadside.

VI. Conclusions

The theory and simulation results presented above suggest that spatial sigma-delta modulation can significantly reduce error in the output of a delay-and-sum beamformer with coarse quantization. The spatial modulators work by shifting the errors introduced by the quantizer in space and time. The resulting spatio-temporal filtering effects can be characterized by the noise transfer functions derived in Section IV. Table I summarizes these NTFs, omitting the $\frac{1}{N}$ terms due to finite array length. The simulation results of Section V suggest that these theoretical NTFs are accurate for first- and second-order spatial modulators, but the quantization error signals on which they act are generally not flat unless the system also includes a temporal modulator.

There are two interpretations of the noise shaping gain functions. As a function of angle, the gains shape the error away from broadside, as in Figure 10. If the array is oversampled in space, i.e. $d \ll \frac{c}{2f}$, then much of the noise can be shaped to $|r| > \frac{d}{c}$, outside the visible region, where it is removed by the delay-and-sum beamformer. The spatial shaping effect is strongest for low frequencies, as shown in Figure 3. In terms of temporal frequency, the gain functions

Architecture	Large-N Noise Shaping Gain
1st-order	$4\sin^2(\frac{\Omega}{2}(\tau+r))$
2nd-order forward	$16\sin^4(\frac{\Omega}{2}(\tau+r))$
2nd-order symmetric	$16\sin^2(\frac{\Omega}{2}(\tau+r))\sin^2(\frac{\Omega}{2}(\tau-r))$
1st-order cascade	$16\sin^2(\frac{\Omega}{2}(\tau+r))\sin^2(\frac{\Omega}{2}\tau)$
2nd-order forward cascade	$64\sin^4(\frac{\Omega}{2}(\tau+r))\sin^2(\frac{\Omega}{2}\tau)$
2nd-order symmetric cascade	$64\sin^2(\frac{\Omega}{2}(\tau+r))\sin^2(\frac{\Omega}{2}(\tau-r))\sin^2(\frac{\Omega}{2}\tau)$

Table I. NOISE SHAPING FOR PROPOSED ARCHITECTURES

shape the error to higher frequencies. For large oversampling ratios, the noise is pushed above the Nyquist rate, where it can be removed by a lowpass filter. This temporal shaping effect is strongest for small r, as in Figure 11, and weaker for larger r, as in Figure 12. Both the spatial and temporal shaping are improved by increasing the spatial oversampling ratio. Meanwhile, the temporal sample rate affects the noise shaping gain of the time-domain stage, if any, and shifts the nulls in the NTF.

The spatial sigma-delta array is most useful in low-frequency applications, such as acoustics, for which the circuit hold times and delays can be made small compared to d/c. In such systems, the internal time delays will not significantly distort the NTFs. Furthermore, if the sample rate is sufficiently high, the delay-and-sum operation can be performed digitally by simply shifting and adding the bit streams. Further work is required to find efficient algorithms and architectures to use these bit streams for beamforming and other directional signal processing, such as direction-of-arrival estimation and source separation. The spatial noise-shaping idea can also be generalized to arbitrary array configurations, such as planar and circular arrays.

Like traditional sigma-delta converters, spatial sigma-delta arrays exploit oversampling to shift quantization noise away from the signal of interest. Such arrays can therefore be constructed with lower-resolution quantizers than conventional systems, reducing constraints on the mixed-signal hardware. By improving resolution and reducing cost, spatial and spatio-temporal sigma-delta modulation can enable novel signal processing architectures for dense wideband arrays.

REFERENCES

[1] H. Van Trees, *Optimum Array Processing*. Detection, Estimation, and Modulation Theory, Wiley, 2002.

[2] E. Larsson, O. Edfors, F. Tufvesson, and T. Marzetta, "Massive mimo for next generation wireless systems," *IEEE Communications Magazine*, vol. 52, no. 2, pp. 186–195, 2014.

[3] A. Mezghani and J. A. Nossek, "On ultra-wideband mimo systems with 1-bit quantized outputs: Performance analysis and input optimization," in *Proc. IEEE Int. Symp. Info. Theory (ISIT)*, pp. 1286–1289, 2007.

[4] M. T. Ivrlac and J. A. Nossek, "On mimo channel estimation with single-bit signal-quantization," in *ITG Smart Antenna Workshop*, 2007.

[5] C. Risi, D. Persson, and E. G. Larsson, "Massive mimo with 1-bit adc," *arXiv:1404.7736*, 2014.

[6] J. Mo, P. Schniter, N. Gonzalez Prelcic, and R. Heath, "Channel estimation in millimeter wave mimo systems with one-bit quantization," in *Asilomar Conf. on Signals, Syst., and Computers*, pp. 957–961, 2014.

[7] G. Zeitler, G. Kramer, and A. Singer, "Bayesian parameter estimation using single-bit dithered quantization," *IEEE Trans. Signal Process.*, vol. 60, pp. 2713–2726, June 2012.

[8] C. Stockle, J. Munir, A. Mezghani, and J. Nossek, "1-bit direction of arrival estimation based on compressed sensing," in *IEEE Int. Workshop on Signal Process. Advances in Wireless Comm. (SPAWC)*, pp. 246–250, June 2015.

[9] Q. Bai and J. A. Nossek, "Design optimization of simo receivers with compact uniform linear arrays and limited precision a/d conversion," in *Proc. Int. ITG Workshop on Smart Antennas (WSA)*, pp. 1–8, 2015.

[10] R. Schreier and G. Temes, *Understanding Delta-Sigma Data Converters*. Wiley, 2005.

[11] D. P. Scholnik, J. O. Coleman, D. Bowling, and M. Nee, "Spatio-temporal delta-sigma modulation for shared wideband transmit arrays," in *Proc. IEEE Radar Conf.*, pp. 85–90, IEEE, 2004.

[12] C.-P. Yeang, G. W. Wornell, L. Zheng, and J. Krieger, "Dense transmit and receive phased arrays," in *Proc. IEEE Int. Symp. Phased Array Syst. and Technol. (ARRAY)*, pp. 934–939, IEEE, 2010.

[13] J. D. Krieger, C.-P. Yeang, and G. W. Wornell, "Dense delta-sigma phased arrays," *IEEE Trans. Antennas and Propagation*, vol. 61, no. 4, pp. 1825–1837, 2013.

[14] M. Brandstein and D. Ward, *Microphone arrays: signal processing techniques and applications*. Springer, 2001.